

Digital Image Plane Holography for Three-Component Velocity Measurements in Turbomachinery Flows

Pilar Arroyo¹, Julia Lobera², Sara Recuero³, Jakob Woisetschläger⁴

1: Instituto de Investigación en Ingeniería de Aragón (I3A), Universidad de Zaragoza, Spain, arroyo@unizar.es

2: Instituto de Investigación en Ingeniería de Aragón (I3A), Universidad de Zaragoza, Spain, jlobera@unizar.es

3: Instituto de Investigación en Ingeniería de Aragón (I3A), Universidad de Zaragoza, Spain, srecuero@unizar.es

4: Institut für Thermische Turbomaschinen und Maschinendynamik, Technische Universität Graz, Austria, jakob.woisetschlaeger@tugraz.at

Abstract Digital Image Plane Holography (DIPH) has been used to record the flow behind a linear turbine blade cascade installed in a transonic wind tunnel. Illuminating the flow with two double-cavity Nd-YAG lasers and using two digital cameras for image recording, a series of digital holograms were taken with one camera while standard PIV recordings were simultaneously taken with the second camera. Both the intensity as well as the phase distribution of the illuminated flow plane were recovered from the holograms. The intensity distribution was used for a standard Particle Image Velocimetry (PIV) evaluation using a time delay of 1 μ s and the two velocity component results are compared with the PIV results obtained from the second camera recordings. The phase distribution was used for a digital speckle pattern interferometry (DSPI) evaluation using a time delay of about 50 ns, which provides out-of-plane velocity component data. Four laser pulses were used to provide the different time delays required by the two analysis techniques. The four flow images were recorded by pairs in each camera frame being the images in each pair taken at the short time interval (50 ns) and the two pairs at the longer time interval (1 μ s). Furthermore, the two flow images in each frame were taken as multiplexed holograms, with the illumination coming from separate lasers, so as to allow an independent reconstruction of the two images. Some results from medium and high speed subsonic flows show the feasibility of using DIPH in turbomachinery flows.

1. Introduction

Digital Image Plane Holography (DIPH) as a fluid velocimetry technique was introduced in 2004 (Lobera et al. 2004a,b) as a further development of digital speckle pattern interferometry (DSPI). DSPI (Andrés et al. 1999) only uses the phase information on the tracer particle scattered light to get information on an out-of-plane fluid velocity component. However, DIPH can use not only the phase but also the intensity so that it can get information on the in-plane fluid velocity components, too. DIPH as a 3-C velocimetry technique has already been demonstrated in a slow convective flow (Lobera et al. 2004b), pointing out the requirement of three temporally separated images due to the higher sensitivity of the phase analysis (DSPI analysis) as compared with the intensity analysis (PIV analysis). For slow flows, where the appropriate time interval for PIV analysis is longer than the frame acquisition time, the 3-C can be measured using only one camera and one continuous laser. For higher speed flows, pulsed lasers with three pulses and two imaging cameras are required for a combined DSPI+PIV analysis (Lobera et al. 2004c). This type of combined analysis has been compared with stereoPIV analysis, showing very good agreement between the two data sets. Let us point out that the two cameras are needed for recording the three temporally separated images because the 3-C can be obtained without the need to have two different observation directions as stereoPIV requires. It has already been shown the influence of the laser temporal coherence length in the size of the measurement region (Andrés et al. 2001) and how to increase that size so that no special laser is required for DIPH.

DIPH has also been shown to work with multiplexed holograms, based on the laser limited

coherence length (Lobera et al. 2004a,b Palero et al 2005). So far, the multiplexed holograms correspond to different fluid planes so that DIPH can work as a quasi 3-D velocimetry technique.

In this paper, DIPH will be demonstrated in a turbomachinery flow that have higher speed, higher noise and less optical access (both for illumination and for observation) than in previous DIPH applications. DIPH will be developed to record a bigger area than in previous applications using only one camera and time intervals shorter than the camera interframing time. A linear arrangement of turbine blades was used as a test object, since a number of previous publications provided reference data for this demonstration at a wide range of Mach and Reynolds numbers (Sieverding and Heinemann, 1990; Woisetschlager et al., 2003). In turbine blade flows the boundary layer material separates from the trailing edge of the turbine blades, forming vortex streets. This vortex shedding influences the aerodynamic performance by affecting the downstream blade rows and is source of noise as well. Therefore, prediction and precise numerical simulation of vortex shedding can aid optimising efficiency and performance of these machines. Novel non-invasive laser-optical techniques can provide additional information and reference data for this optimisation process.

2. Digital Image Plane Holography (DIPH) as a 3-C Velocimetry Technique

2.1 Recording setup

In DIPH, a fluid plane is illuminated with a laser sheet and it is imaged onto the CCD sensor, like in standard PIV. Being a holographic technique, a reference beam coherent with the light coming from the fluid plane (object beam) is also required. In DIPH, this reference beam is a divergent beam whose focus is in the same plane as the fluid imaging system. This type of reference beam minimizes the local angle between the object and reference beams, which minimizes the limitations imposed by the low spatial resolution of the CCD sensors where the hologram is being recorded. DIPH can be implemented with the same double cavity Nd-YAG lasers normally used for PIV but their main drawback is that their temporal coherence length is short, on the order of 10 mm. Thus, special care has to be taken in matching (within 10 mm) the optical path lengths of the object and reference beams so that they are able to interfere in the sensor plane, which is essential for recording a hologram.

Figure 1 shows the DIPH recording setup implemented to observe the flow inside a transonic wind tunnel with 100x230 mm cross-section. A beam from a NewWave Gemini laser was sent to the flow through a light guiding arm (LGA). A probe at the end formed a light sheet in the flow area, impinging from the exit flow direction. The laser, the input to the light guiding arm, the reference beam and camera 1 were arranged on top of a heavy and vibration isolated table placed next to wind tunnel. Optical access for imaging the flow was granted by two flat glass windows of 100x180 mm size and 15 mm thickness. The reference beam was obtained by diverting a small amount of the laser with an uncoated wedge (WBS). The reflection from the first surface was made to travel a long path (about the same distance as the LGA length) by means of a 40 mm side rectangular prism (P) and two mirrors (M_1 and M_2). The reference beam path length can be easily changed by displacing the prism. Two linear polarizers are used to control the reference beam intensity while maintaining the correct beam polarization. A short focal length ($f=20$ mm) converging lens and a non polarizing 20/80 beamsplitter were used to produce the divergent beam at the right position with the correct incidence angle. Everything was covered with a foam/wood frame to reduce the noise-induced-vibration produced when the compressor is in operation. Another camera (camera 2), placed on the other side of the wind tunnel, was used for standard PIV

recordings. Two Lavision Imager Pro 4008x2672 pixel cameras were set to record the same common area of 36.1 mm in width by 54.1 mm in height.

All tests were performed in a linear arrangement of seven VKI-1 turbine profiles (Kiock et al., 1986) installed into the wind tunnel. Air was continuously supplied by a centrifugal-compressor, which was part of the institute compressor station at Graz University of Technology (Pirker et al., 1995). Blade chord length was 58 mm, blade height 100 mm (equals channel height), spacing of

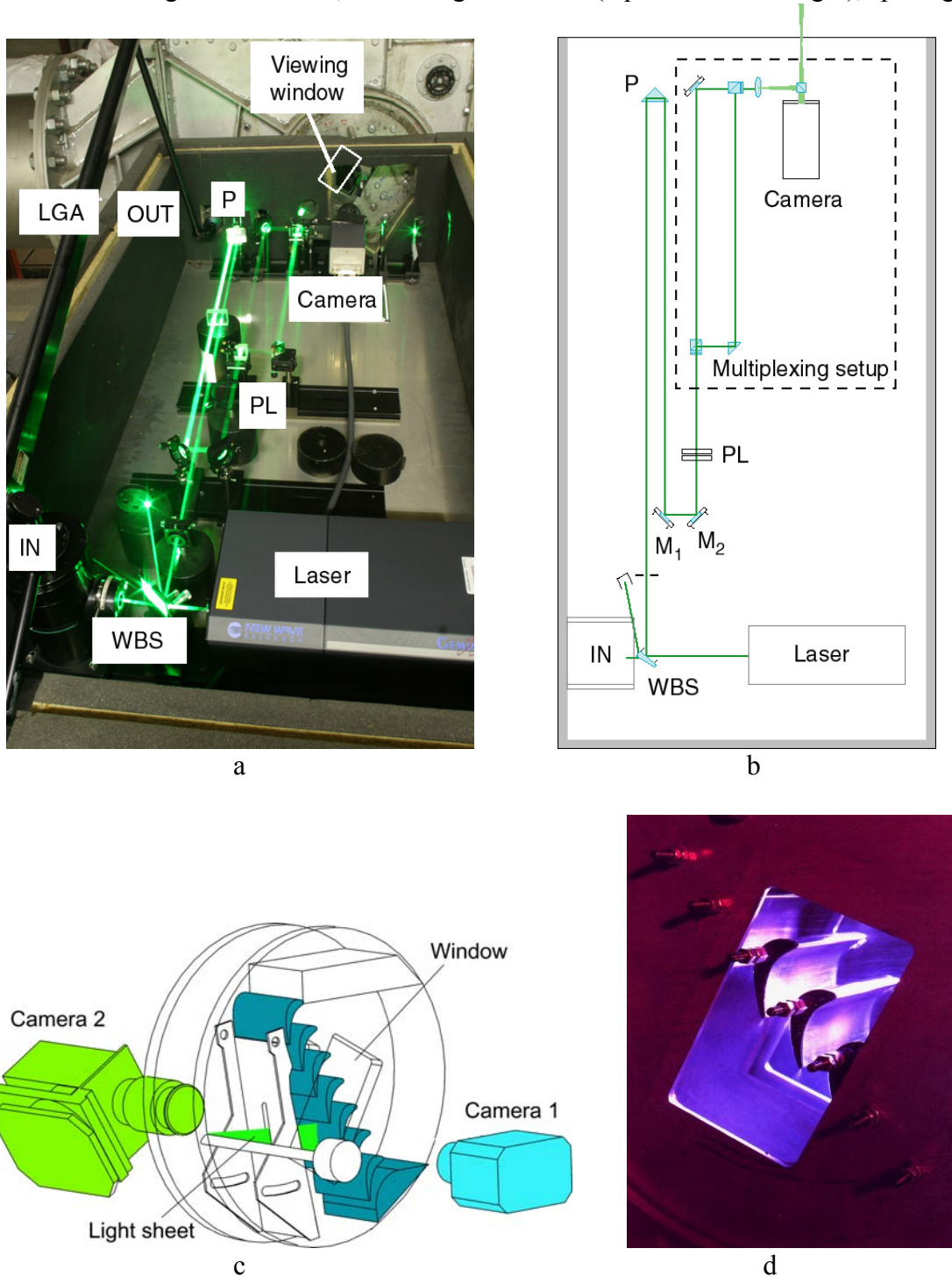


Fig. 1. a) Diph setup in the cascade flow; b) Reference beam setup; c) Flow area and recording cameras; d) Closer view of the cascade blades and the viewing window. (WBS: wedge beam splitter; IN: input to the light guiding arm; LGA: light guiding arm; OUT: coupling of the light guiding arm with the flow area; P: prism; PL: liner polarizers; M_1 , M_2 : mirrors)

blades 41.2 mm and trailing edge thickness 2.9 mm. Flow inlet and outlet conditions were recorded by a 16-channel pressure-scanner ZOC14/16Px-50psid (Scanivalve) and amplifiers for 7 thermocouples. Accuracy for the standard instrumentation was 0.08% or 280 Pa for the pressure scanner and 1 K for the temperature measurement. Exit flow Mach number M was calculated using isentropic relations, total temperature and total pressure at inlet conditions, as well as, static pressure at outlet conditions (Bölcs and Suter, 1986). Reynolds number Re and Strouhal number Str were based on the isentropic exit velocity and viscosity at isentropic exit conditions. Characteristic length for Re was the chord length and for Str the trailing edge thickness. During data recording Mach and Reynolds numbers were continuously displayed to control the compressor station. Seeding was provided by two Palas AGF 2.0D particle generator 1 m in front of the turbine blade cascade through an 8 mm pipe, operated at 0.5 to 1 bar over-pressure. DEHS (Diethylexylsebacat) was used as seeding material. According to the manufacturer, a mean droplet size of approximately $0.3 \mu\text{m}$ is measured immediately after the cyclone of the particle generator.

2.2 Hologram analysis

Figure 2a shows a typical DIPH recording (digital hologram) where only the reference beam is seen since its intensity is about 10 times bigger than the object mean intensity. It shows the non uniform beam shape typical of standard Nd-YAG lasers. It also shows some low frequency modulation due to unwanted (and difficult to remove) reflections on the reference beam. The modulation produced by the interference of the object and reference beams is of much higher spatial frequency and it is made evident in the frequency power spectrum (fig. 2b).

The analysis of digital holograms always involves the reconstruction of the object. In DIPH, where the object is the fluid plane and its image is on the digital sensor, our aim is to reconstruct both the phase and the intensity of the image. Being an image plane hologram, all the terms of the reconstruction (object intensity, reference intensity, virtual image and real image) are overlapped. However, with our recording setup, the holograms are also lensless Fourier holograms of the imaging system aperture. Thus, a simple Fourier transform provides a reconstruction of the beams at the plane where the origin of the reference beam was. In this plane, the real and virtual images of the aperture are spatially separated as the Fourier plane intensity (power spectrum) shown in figure 2b demonstrates. After selecting one of the aperture images, displacing it to the Fourier plane center and calculating the inverse Fourier transform of the complex function, the fluid plane image intensity (fig. 2c) and phase (fig 2d) are recovered. The subtraction of two phase maps (DSPI analysis) obtained from two holograms taken with a short time interval produces a fringe map (fig. 2e) which represents an isoline map for an out-of-plane velocity component. The component lies along a direction at 45° with the light sheet and each fringe represent a change of $0.4 \mu\text{m}$ in the fluid displacement along that direction. Figure 2e also shows the size of the region where a hologram was effectively recorded. Outside that area, the difference in optical path length between the reference and object beams was longer than the laser temporal coherence length. The same limitation in the measurement region is seen in figure 2c, where the object intensity is only reconstructed in the coherent area. Furthermore, the intensity reconstructed is not just the object intensity but the product of the object and reference intensities. This is the reason why the reconstructed intensity does not fill a rectangular area but a curved one with a shape similar to the brightest area of the reference beam. The corresponding PIV recording taken with camera 2 (fig. 2e) shows there was no problem with the seeding, which was good and uniform. By applying a standard PIV analysis to two intensity maps obtained from two holograms taken with a longer time interval, the two in-plane velocity components are calculated. Thus, all the three velocity components can be measured from the holograms recorded with camera 1, being camera 2 recordings only taken as an extra help in the DIPH implementation.

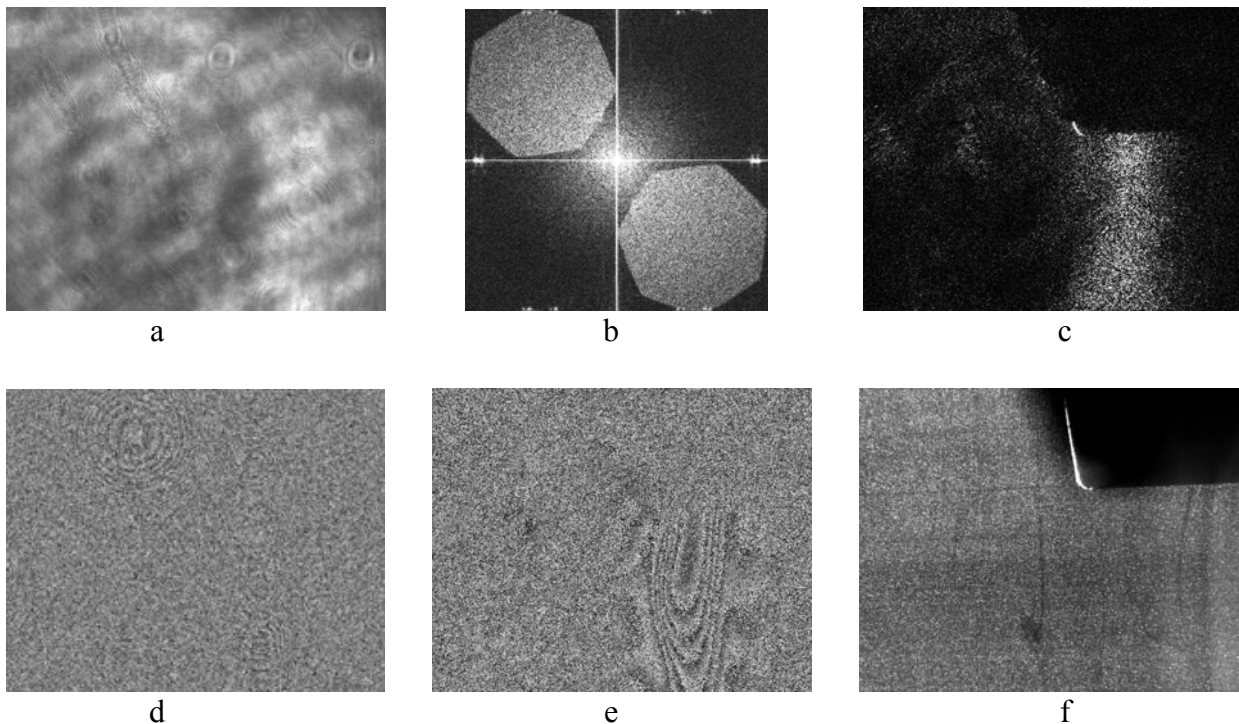


Fig. 2. Digital hologram (a) taken with camera 1 and some results from its analysis: b) Intensity reconstructed in the aperture/reference beam source plane; c) Object intensity reconstructed in the image plane. d) Object phase reconstructed in the image plane; e) Object phase difference map obtained from subtracting two phase maps. f) Corresponding PIV image taken with camera 2.

3. Multiplexing setup

DIPH as a 3-C velocimetry technique requires at least three images due to the different sensitivity of the phase and intensity map analysis: DSPI analysis requires displacements smaller than one pixel while PIV analysis requires displacements of a few pixels. For this reason, all the results shown in the following have been obtained with two double cavity Nd-YAG lasers. The lasers have been combined, prior to the WBS, by using a high energy polarizing beamsplitter cube. The first pulse of each laser has been recorded in the first frame of the two cameras while the second pulse of the two lasers have been recorded in the second frame of the cameras (fig. 3). Time intervals of $t_L=1 \mu\text{s}$ have been set for each double cavity laser while the two lasers were fired with a relative delay of $t_S=50 \text{ ns}$. In order to separate the four images, two holograms have been multiplexed in each frame recording. This multiplexing also allowed to use time intervals shorter than the minimum camera interframing time

The reference beam setup (fig. 4) was also adapted so that a longer measurement region could be used.

3.1 Extension of measurement region

The extension of the measurement region is based on overlapping four beams with different optical path lengths. The beam R is divided into beams R0 and R1 with a 50/50 non polarizing beamsplitter cube (NPBS1). The path length for R1 will be longer than for R0 because its reflection is produced by a glass prism P1 while R0 is reflected by a mirror M1. The goal is that the optical path length difference between R1 and R0 matches the laser temporal coherence length, which is

about 10 mm. For a perfectly perpendicular arrangement, the difference in optical path length will be $(n-1)L$ being n and L the glass refraction index and the prism side length. A 25 mm prism will introduce a difference of about 12.5 mm. However, the arrangement is very versatile and the path length difference between R1 and R0 can be easily modified by changing the perpendicularity of the arrangement (the mirror M1 can be moved closer or further apart from the beamsplitter NPBS2). A second 50/50 non polarizing beamsplitter (NPBS2) divides both R0 and R1 into two beams following different paths. We keep the names R0 and R1 for the beams that are reflected in mirror M2 while beams R2 and R3 are reflected with a prism P2 whose length should be such that it introduces an optical path length about twice the laser coherence length. A 40 mm side prism has been used for this purpose.

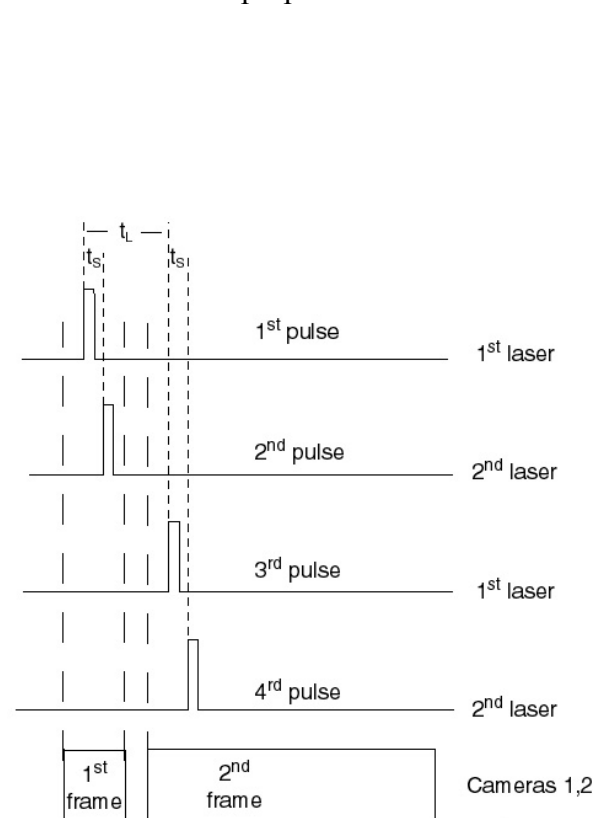


Fig. 3. Synchronization diagram

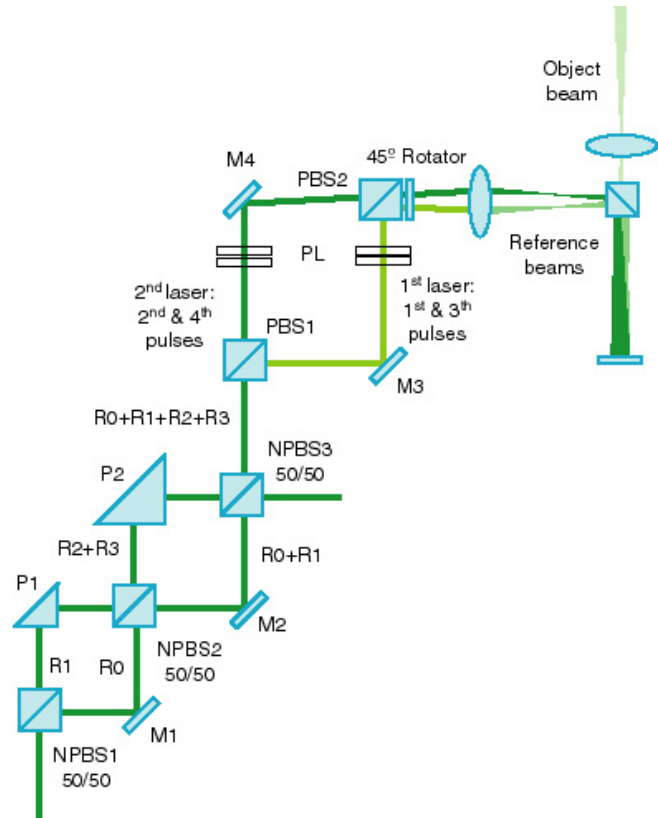


Fig. 4. Reference beam setup

3.2 Decreasing the minimum time interval

In the next step the reference beams for each of the two lasers are separated using a low energy polarizing beam splitter cube. These reference beams travel through different paths allowing to produce two divergent reference beams with their origin in different positions. The intensity of these two reference beams is controlled by a pair of linear polarizers, PL. Each reference beam will interfere only with the object beam coming from the same laser as the reference beam. Thus the two holograms in each frame will allow to reconstruct the object wave in two different time instants, whose interval can be as short as required because the pulses come from different lasers. However, if the required time intervals are shorter than 10 times the laser pulse width we will run into time average holography problems. The time interval between the pulses from the same laser will be limited by the camera interframing time since they have to be recorded in separate frames. Figure 5 shows the four aperture images obtained from reconstructing each multiplexed hologram. By selecting the appropriate aperture image, the corresponding object wave will be reconstructed as explained before.

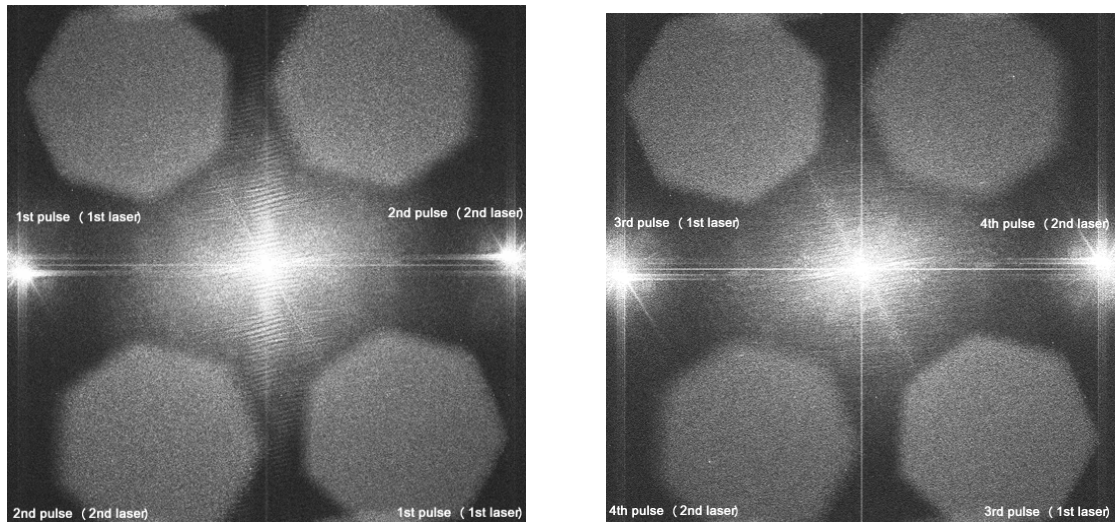


Fig.5 Frequency power spectrum of the multiplexed holograms. Shown are the first frame (left) and the second frame (right) recorded with the two Nd-YAG laser systems and camera 1.

3.3 Demonstration in a natural (slow) flow

DIPH with the described multiplexing setup was first tested in the natural flow that occurs in the wind tunnel when the compressor is switched off. Figure 6 shows the phase difference maps obtained from comparing different pairs of images from the four available images. The map corresponding to second – first images (fig. 6a) or fourth-third images should show the flow displacement for a very short time interval ($t_s = 50$ ns), which should be negligible. The maps corresponding to third-first (fig. 6b), fourth-second (fig. 6c) and fourth-first (fig. 6d) images should show the flow displacement for a longer time interval ($t_L = 1$ μ s), which is not negligible. Figures 6b and 6c are pretty similar as they are taken with a delay of only 50 ns between them. By subtracting the phase map of figures 6d and 6a a map similar to that of figures 6b and 6c is obtained. This demonstrates that the fringe pattern of figure 6a, whose origin is related to the fact that the two reference beams follow different paths, can be considered a background pattern that has to be removed from any phase map that compares two images from different lasers.

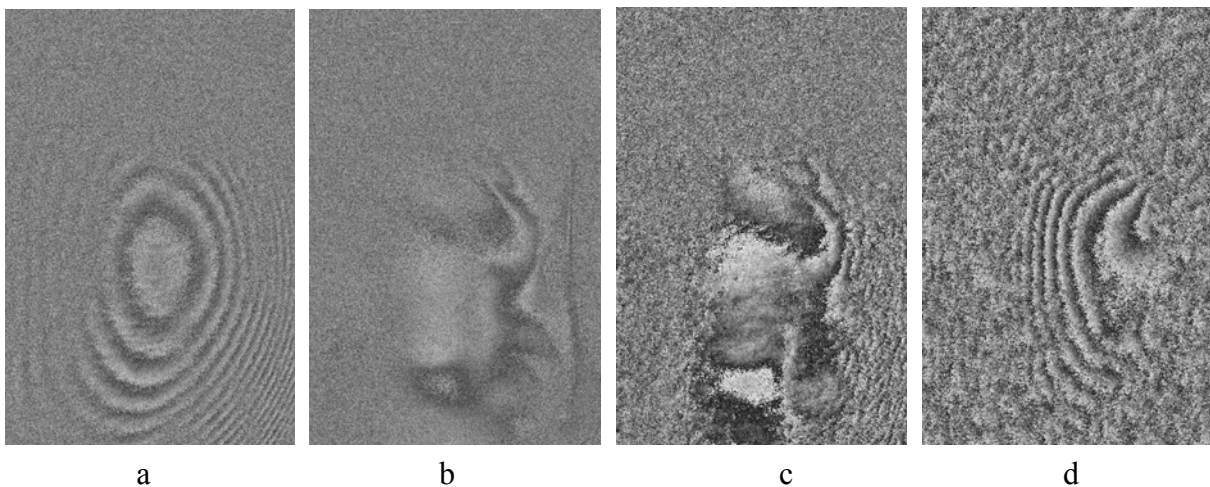


Fig.6: Phase maps obtained from the DIPH holograms. a) 1st and 2nd pulse recorded within the 1st frame. b) 1st and 3rd pulse recorded within the 1st and 2nd frame. c) 2nd and 4th pulse recorded within 1st and 2nd frame (low-pass filtered within the frequency domain). d) 1st and 4th pulse recorded within 1st and 2nd frame (low-pass filtered within the frequency domain).

Figure 7 compares the images for PIV evaluation obtained from a DIPH hologram taken with camera 1 and from the PIV recording taken with camera 2. The images taken by camera 2 have better signal to noise ratio and thus they should produce higher spatial resolution measurements. However, a proper PIV evaluation and comparison cannot be made since the time interval is too short.

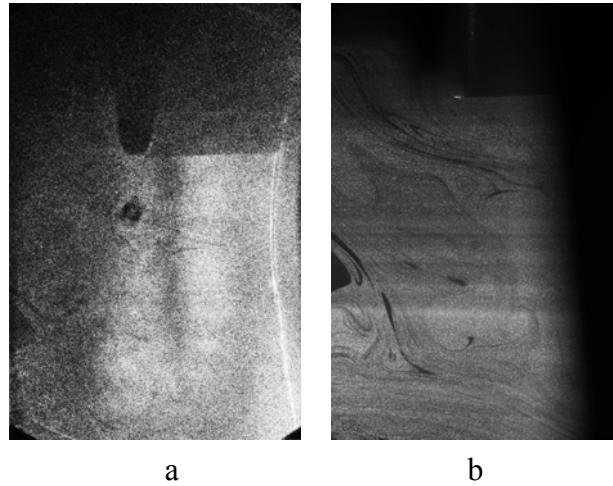


Fig.7 Images for PIV evaluation obtained from: a) the DIPH holograms taken with camera 1; b) camera 2 used for PIV recordings only.

4. Results from the wake of turbine blades

Figures 8 and 9 shows some results obtained from two different flow conditions. The purple rectangle shows the area than can be analyzed in camera 1 and its corresponding position in the images taken with camera 2. The vertical line marks the center of the blade producing the wake being recorded. The next blade is on the right side of the measurement region (black area on the right of figs 8, 9 b and no vector area on the right of figs 8, 9 a).

The phase map difference shows a smaller displacement for the lower Ma flow (fig. 8c) than for the higher Ma flow (fig. 9c) as expected. In both cases the maximum displacement is too small since there is less than one fringe at Ma=0.20 and about one fringe at Ma=0.40. A time interval several times longer than 50 ns would have been more appropriate. The PIV recordings taken with camera 2 (figs. 8, 9 b) shows that the seeding is not uniform although it does not affect to the phase maps as we have already observed in previous experiments. Although not uniform, there is enough seeding for the PIV analysis to produce correct in-plane vector data (figs. 8, 9 a) in the whole plane. The V_x measured from PIV recordings is also shown as an isoline map for 0.8 pixel intervals. This 0.8 pixel displacement for a time interval of 1 μ s corresponds to a displacement of 0.5 μ m for a time interval of 50 ns. If we neglect the V_z component, each fringe in the phase difference maps would correspond to a displacement change of 0.5 μ m. The phase maps have less fringes than what this PIV data indicates. This can be due either to low spatial resolution, which we do not believe is the case, or to an incorrect value of the time interval. We believe the time interval might not have been 50 ns because 50 ns was the time resolution of our synchronizer which means the value might not be accurate enough.

5. Conclusions

Some new developments of DIPH as a 3-C velocimetry technique have been presented. They include the first application of DIPH to a turbomachinery flow, a modified reference beam for

overcoming the limitation in the measurement region size imposed by the short coherence length Nd-YAG lasers and a new multiplexing setup for using only one camera and shorter time intervals than the camera interframing time in the 3-C measurement process. DIPH qualitative information compares well with the simultaneous velocity measurements obtained with digital PIV.

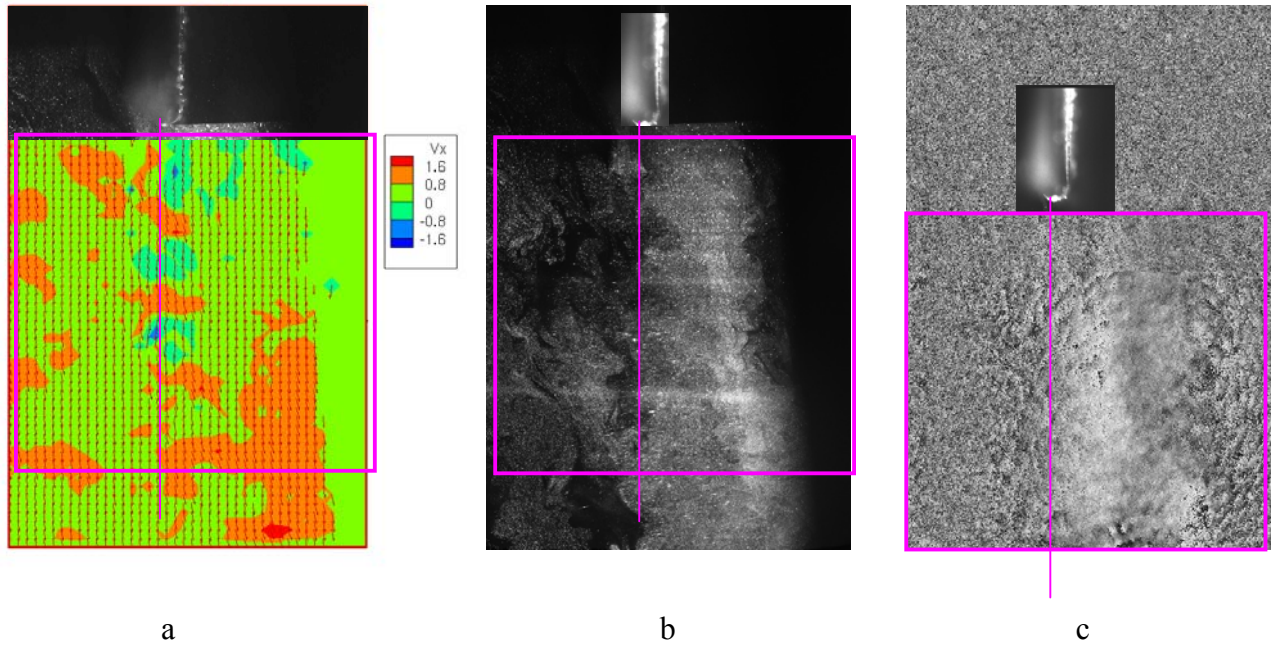


Fig. 8. Some results from a flow at $Ma=0.20$. a) Vector map and isoline map obtained from the PIV images; b) PIV image from camera 2; c) Phase difference map from holograms.

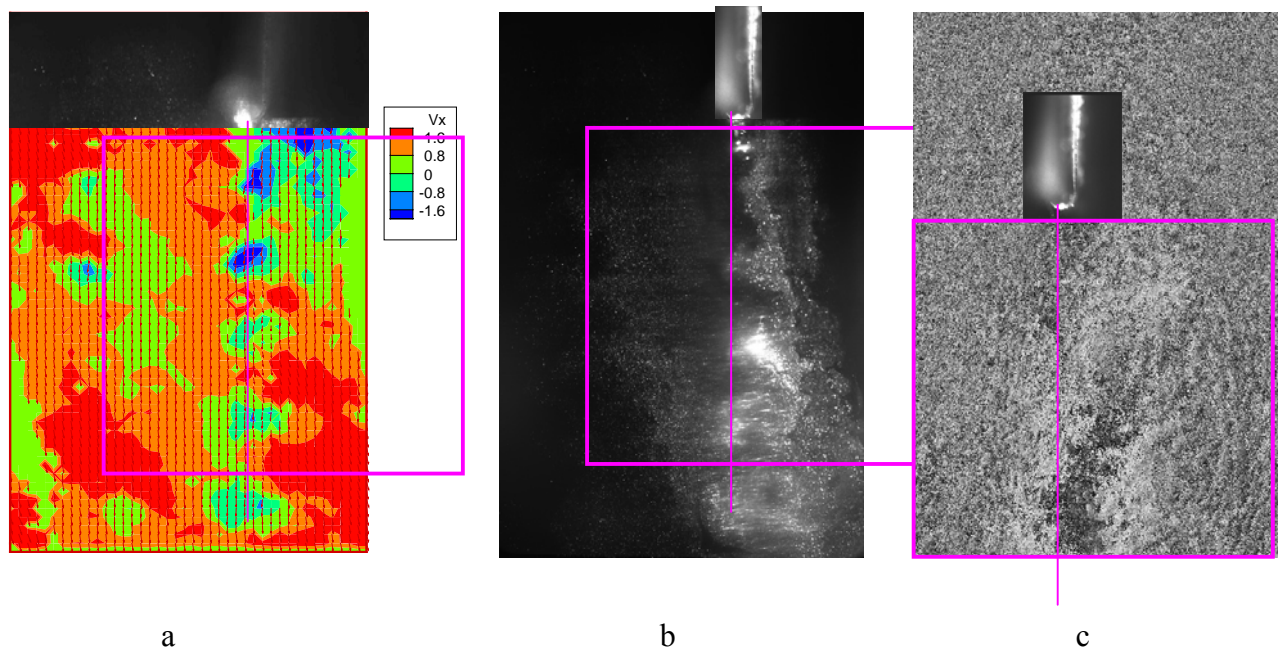


Fig. 9. Some results from the flow at $Ma=0.43$. a) Vector map and isoline map obtained from the PIV images; b) PIV image from camera 2; c) Phase difference map from holograms.

Acknowledgements

This project was supported by the Spanish-Austrian Cooperation Program 2004-2005 (Acciones Integradas) within grants HU2003-0028 Ministerio de Ciencia y Tecnología and 22/2004 Österreichischer Austauschdienst ÖAD. This research was further supported by the Ministerio de Ciencia y Tecnología (DPI2003-06725-C02-02) and by the Diputación General de Aragón (G.I.A. T63 Tecnología Óptica Laser). The support of Prof. Peter Pirker and Oliver Schennach, both from Graz University of Technology, in the operation of the compressor station and the test rig is gratefully acknowledged.

References

- Andrés, N, Arroyo MP, Hinrichs H, Quintanilla M** (1999) Digital speckle-pattern interferometry as a full-field-velocimetry technique. *Opt. Lett.*, **24**, 575-577
- Andrés N, Arroyo MP, Zahn H, Hinrichs H** (2001) Application of digital speckle pattern interferometry for fluid velocimetry in wind tunnel flows. *Exp in Fluids* 30:562-567
- Bölcs A, Suter P** (1986) *Transsonische Turbomaschinen*, G.Braun, Karlsruhe
- Lobera J, Andrés N, Arroyo MP**, (2004a) "Digital speckle interferometry as a holographic velocimetry technique", *Meas. Sci. Technol.* 15, 718-724
- Lobera J, Andrés N, Arroyo MP** (2004b) From ESPI to Digital Image Plane Holography (DIPH): requirements, possibilities and limitations for velocity measurements in a 3-D region. In *Particle Image Velocimetry: Recent Improvements Proc. EUROPIV 2 Workshop on Particle Image Velocimetry (Zaragoza)* Eds. M. Stanislas, J. Westerweel, J. Kompenhans, 363-372
- Lobera J, Arroyo MP, Perenne N, Stanislas M** (2004c) Comparison between PIV&ESPI and Stereo PIV on the measurement of 3-C velocity fields. In *Particle Image Velocimetry: Recent Improvements Proc. EUROPIV 2 Workshop on Particle Image Velocimetry (Zaragoza)* Eds. M. Stanislas, J. Westerweel, J. Kompenhans, 351-361
- Kiock R, Lehthaus F, Baines NC, Sieverding CH** (1986) The Transonic Flow Through a Plane Turbine Cascade as Measured in Four European Wind Tunnels, *ASME Journal of Engineering for Gas Turbines and Power*, 108:277-284
- Palero V, Lobera J, Arroyo MP** (2005) Digital Image Plane Holography (DIPH) for two-phase flow diagnostics in multiple planes. *Exp.in Fluids* 39: 397-406
- Pirker HP, Jericha H, Zhuber-Okrog G** (1995) Auslegung und Betriebsverhalten einer Verdichteranlage für die Luftversorgung wissenschaftlicher Versuchseinrichtungen, *VDI Berichte* 1208:331-347
- Sieverding CH, Heinemann H** (1990) The Influence of Boundary Layer State on Vortex Shedding From Flat Plates and Turbine Cascades, *ASME Journal of Turbomachinery*, 112:181-187
- Woisetschläger J, Mayrhofer N, Hampel B, Lang H, Sanz W**, (2003) Laser-optical investigation of turbine wake flow, *Exp.Fluids* 34:371-378